



# Compact Binary Mergers and the Event Rate of Fast Radio Bursts

Xiao-Feng Cao<sup>1</sup>, Yun-Wei Yu<sup>2,3</sup> , and Xia Zhou<sup>4</sup><sup>1</sup> School of Physics and Electronics Information, Hubei University of Education, Wuhan 430205, People's Republic of China<sup>2</sup> Institute of Astrophysics, Central China Normal University, Wuhan 430079, People's Republic of China; [yuyw@mail.ccnu.edu.cn](mailto:yuyw@mail.ccnu.edu.cn)<sup>3</sup> Key Laboratory of Quark and Lepton Physics (Central China Normal University), Ministry of Education, Wuhan 430079, People's Republic of China<sup>4</sup> Xinjiang Astronomical Observatory, Chinese Academy of Sciences, Urumqi 830011, People's Republic of China*Received 2017 November 18; revised 2018 February 25; accepted 2018 March 27; published 2018 May 10*

## Abstract

Fast radio bursts (FRBs) are usually suggested to be associated with mergers of compact binaries consisting of white dwarfs (WDs), neutron stars (NSs), or black holes (BHs). We test these models by fitting the observational distributions in both redshift and isotropic energy of 22 Parkes FRBs, where, as usual, the rates of compact binary mergers (CBMs) are connected with cosmic star formation rates by a power-law distributed time delay. It is found that the observational distributions can well be produced by the CBM model with a characteristic delay time from several tens to several hundreds of megayears and an energy function index  $1.2 \lesssim \gamma \lesssim 1.7$ , where a tentative fixed spectral index  $\beta = 0.8$  is adopted for all FRBs. Correspondingly, the local event rate of FRBs is constrained to  $(3-6) \times 10^4 f_b^{-1} (\mathcal{T}/270 \text{ s})^{-1} (\mathcal{A}/2\pi)^{-1} \text{ Gpc}^{-3} \text{ yr}^{-1}$  for an adopted minimum FRB energy of  $E_{\min} = 3 \times 10^{39} \text{ erg}$ , where  $f_b$  is the beaming factor of the radiation,  $\mathcal{T}$  is the duration of each pointing observation, and  $\mathcal{A}$  is the sky area of the survey. This event rate, about an order of magnitude higher than the rates of NS-NS/BH-NS mergers, indicates that the most promising origin of FRBs in the CBM scenario could be mergers of WD-WD binaries. Here a massive WD could be produced since no FRB was found to be associated with an SN Ia. Alternatively, if all FRBs can repeat on a timescale much longer than the period of current observations, then they could also originate from a young active NS that forms from relatively rare NS-NS mergers and accretion-induced collapses of WD-WD binaries.

*Key words:* radio continuum: general – stars: neutron – white dwarfs

## 1. Introduction

Studies on mergers of binary systems composed of a pair of compact objects, i.e., white dwarfs (WDs), neutron stars (NSs), or black holes (BHs), are of fundamental importance in astrophysics, because these mergers have or might have tight connections with current and future detections of gravitational waves (Abbott et al. 2016, 2017), with the formation of heavy elements via the r-process (Lattimer & Schramm 1974; Eichler et al. 1989; Bauswein et al. 2013; Hotokezaka et al. 2013; Just et al. 2015), with the production of type Ia supernovae (SNe Ia; Tutukov & Yungelson 1981; Webbink 1984; Wang & Han 2012), and with the origin of short gamma-ray bursts (GRBs; Paczynski 1986; Eichler et al. 1989; Guetta & Piran 2006; Coward et al. 2012) as well as mergernova/kilonova emission (Li & Paczyński 1998; Metzger et al. 2010; Yu et al. 2013; Coulter et al. 2017; Evans et al. 2017). The detection of various possible electromagnetic radiation from compact binary mergers (CBMs) can play a crucial role in uncovering the nature of progenitor binaries and in locating and identifying the associated gravitational wave signals.

Recently, it was suggested that some CBMs, specifically, mergers of double WDs (Kashiyama et al. 2013), of double NSs (Totani 2013; Wang et al. 2016; Yamasaki et al. 2017), of an NS and a BH (Mingarelli et al. 2015), or even of two charged BHs (Liu et al. 2016; Zhang 2016), could be responsible for the newly discovered fast radio bursts (FRBs). FRBs are millisecond radio transients of intensities of a few to a few tens of jansky at  $\sim 1 \text{ GHz}$  (Lorimer et al. 2007; Keane et al. 2012, 2016; Thornton et al. 2013; Burke-Spolaor & Bannister 2014; Spitler et al. 2014; Masui et al. 2015; Ravi et al. 2015; Champion et al. 2016; Bannister et al. 2017; Caleb et al. 2017; Petroff et al. 2017). Due to the short durations of

FRBs and the low angular resolution of present radio surveys, it is difficult to capture counterparts of FRBs in other wavelength bands, even if these counterparts indeed exist. This makes it impossible to directly determine the distances of FRBs<sup>5</sup> and to identify their origins. In any case, the anomalously high dispersion measures (DMs;  $\sim 200-2600 \text{ pc cm}^{-3}$ ) of FRBs, which are too high to be accounted for by the high-latitude interstellar medium in the Milky Way, robustly suggest that the FRBs could have cosmological distances of redshifts up to  $z \sim 4.0$ . Therefore, the isotropically equivalent energy release of an FRB can be estimated to within the range of  $\sim 10^{39-42} \text{ erg}$ . In the suggested CBM models, such an energy could be naturally provided by the inspiral of the binary or the spin-down of the remnant object due to magnetic dipole radiation and magnetospheric activities. Furthermore, it is believed that this energy should be released via coherent radiations, with some similarity to the pulse radiation of pulsars (Yang & Zhang 2017a).

Besides the energy scale and timescale of FRBs, another crucial constraint on any model is the event rate of FRBs and, furthermore, its redshift dependence. During the past several years, the increasing FRB number has already enabled a statistical investigation of FRBs (Yu et al. 2014; Bera et al. 2016; Caleb et al. 2016; Katz 2016a, Li et al. 2017; Lu & Kumar 2016; Oppermann et al. 2016; Vedantham et al. 2016; Cao et al. 2017a; Fialkov & Loeb 2017; Lawrence et al. 2017; Cao & Yu 2018; Macquart & Ekers 2018). In particular, Cao et al. (2017a) found that the proportional

<sup>5</sup> For the only repeated FRB, FRB 121102, its host galaxy and a persistent radio counterpart have been detected and then its redshift has been measured to  $z = 0.19$ , which undeniably confirmed its cosmological origin (Chatterjee et al. 2017; Marcote et al. 2017; Tendulkar et al. 2017).

coefficient between the FRB rates and cosmic star formation rates (CSFRs) could be redshift-dependent, which somewhat favors the CBM model. Therefore, in this paper, we confront the CBM model with the number distributions of FRBs in redshift as well as in energy (see Yamasaki et al. 2017 for a relevant calculation). By fitting the observational distributions, we test the feasibility of the CBM model for explaining the FRB phenomena and, simultaneously, constrain the model parameters. According to the observational constraints, the possible nature of the progenitor compact binaries can be discussed.

## 2. The Model

### 2.1. The Rate of CBMs

A merger takes place after a compact binary loses its orbital energy through gravitational radiation. The rate of CBMs at redshift  $z$  can be related to the CSFR at redshift  $z'$  that is determined by the time delay equation as  $t(z') = t(z) - \tau$ , where  $t(z) = \int_z^\infty [(1+z')H(z')]^{-1} dz'$  is the age of the universe at redshift  $z$  and  $H(z) \equiv H_0 \sqrt{\Omega_M(1+z)^3 + \Omega_\Lambda}$ . Hereafter, the cosmological parameters are taken as  $\Omega_M = 0.32$ ,  $\Omega_\Lambda = 0.68$ , and  $H_0 = 70 \text{ km s}^{-1} \text{ Mpc}^{-1}$ . The delay time  $\tau$  is determined by both the gravitational radiation decay of the binary orbit and the formation process of the compact binary. The latter factor is further related to the supernova mechanism, the natal kick velocity of NS, the mass transfer between the binary stars, etc. (e.g., Portegies Zwart & Yungelson 1998; Belczynski et al. 2002; Mennekens et al. 2010; Chruslinska et al. 2018). By considering a probability distribution of  $P(\tau)$  of the delay times, the rate of CBMs can be calculated by the following convolution (Piran 1992; Guetta & Piran 2006):

$$\begin{aligned} \dot{R}_m(z) &\propto \int_0^{t(z)-t(z_b)} \dot{\rho}_* [t(z) - \tau] P(\tau) d\tau \\ &\propto \int_z^{z_b} \dot{\rho}_*(z') P[t(z) - t(z')] \frac{dt}{dz'} dz', \end{aligned} \quad (1)$$

where  $\dot{\rho}_*(z)$  is the CSFR and  $dt/dz = -[(1+z)H(z)]^{-1}$ . The upper limit of the above integrate,  $z_b$ , is set at the redshift when the binaries start forming.

Following a series of measurements of CSFRs, a consensus on the history of cosmic star formation emerges up to redshift  $z \sim 4$  (Hopkins & Beacom 2006). In the Hopkins & Beacom's data, a trend of decrease of the CSFRs appears in the higher redshift range. This trend was further confirmed by the observations of Lyman break or Ly $\alpha$  emitter galaxies (Bouwens et al. 2012, 2015; Coe et al. 2012; Oesch et al. 2013, 2014; McLeod et al. 2016) and long GRBs (Chary et al. 2007; Yüksel et al. 2008; Kistler et al. 2009; Wang & Dai 2009; Ishida et al. 2011; Tan et al. 2015), although there is still a debate on the decrease rate at high redshifts. The high-redshift CSFRs can also be constrained by the Gunn–Peterson trough observations to quasars and by the Thomson scattering optical depth of cosmic microwave background photons (e.g., Yu et al. 2012; Wang 2013). Combining the various measurements and constraints, we take the cosmic star formation history as

follows (Yu et al. 2012):

$$\dot{\rho}_*(z) \propto \begin{cases} (1+z)^{3.44}, & \text{for } z < 0.97, \\ (1+z)^0, & \text{for } 0.97 \leq z < 3.5, \\ (1+z)^{-0.8}, & \text{for } z \geq 3.5, \end{cases} \quad (2)$$

with a local CSFR of  $\dot{\rho}_*(0) = 0.02 M_\odot \text{ yr}^{-1} \text{ Mpc}^{-3}$ . In any case, the uncertainty of the high-redshift CSFRs would not significantly influence the rates of CBMs at relatively low redshifts of most FRBs.

The lifetime of gravitational radiation decay of a binary orbit is determined by the initial orbital separation ( $a_i$ ) and the initial ellipticity ( $e_i$ ). According to the relation  $\tau \propto a_i^4$  and assuming  $P(a_i) \propto a_i^q$ , Piran (1992) suggested

$$P(\tau) = P(a_i) \frac{da_i}{d\tau} \propto \tau^{(q-3)/4}, \quad (3)$$

where the initial ellipticity is taken as a constant. A reference value of  $q = -1$  can further be inferred from the data of regular binaries, which yields

$$P(\tau) \propto 1/\tau. \quad (4)$$

On the one hand, this simple power-law distribution has been generally confirmed by more elaborate calculations (e.g., Greggio 2005; Belczynski et al. 2006; Mennekens et al. 2010; Ruitter et al. 2011; Mennekens & Vanbeveren 2016). This indicates that delayed times are dominated by the gravitational radiation. On the other hand, such a delay time distribution has been widely and successfully applied in modeling the redshift distribution of SNe Ia originating from mergers of double WDs (Totani et al. 2008; Maoz & Mannucci 2012) and of short GRBs originating from mergers of double NSs or an NS and a BH (Guetta & Piran 2006; Nakar et al. 2006; Virgili et al. 2011; Hao & Yuan 2013; Wanderman & Piran 2015). Furthermore, this power-law distribution could also be supported by the observations of six double NS systems (Champion et al. 2004).

The delay time distribution is usually found to be peaked at a cutoff value,  $\tau_c$ , below which the probability decreases drastically. Therefore, we tentatively take an empirical expression as follows:

$$P(\tau) \propto \left(\frac{\tau}{\tau_c}\right)^{-1} e^{-\tau_c/\tau}, \quad (5)$$

with which we derive the CBM rate as a function of redshift from Equation (1). The result is primarily dependent on the value of the crucial cutoff of the delay times, as presented in Figure 1. Numerical simulations show that the value of  $\tau_c$  is probably around a few hundred megayears for double NS mergers, but around a few tens of megayears for NS–BH mergers (Mennekens & Vanbeveren 2016; Chruslinska et al. 2018). The delay time distribution of SNe Ia can usually be described by a broken power law consisting of  $\tau^{-0.5}$  and  $\tau^{-1}$  (Greggio 2005; Graur & Maoz 2013), where the former power law is probably determined by the formation time of WDs. Therefore, the value of  $\tau_c$  for double WD mergers can, in principle, be defined by the break time between the two power laws, which also ranges from several tens to several hundreds of megayears.

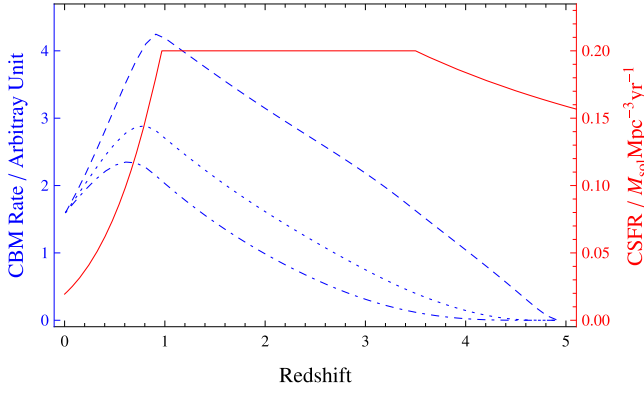


**Figure 1.** CBM rate as a function of redshift for different characteristic delay times:  $\tau_c = 100, 500,$  and  $1000$  Myr (dashed, dotted, and dashed–dotted lines, respectively), where  $z_b = 5$  is taken. The solid line represents the adopted star formation history.

## 2.2. Model-predicted FRB Numbers

It is assumed that a particular type of CBM produces the observed FRBs of isotropic energy releases of  $E$ , which could satisfy a power-law distribution as

$$\Phi(E) \equiv \frac{dN}{dE} \propto E^{-\gamma}, \text{ for } E \geq E_{\min}, \quad (6)$$

where the value of  $E_{\min}$  can roughly be inferred from observations. The combination of the above intrinsic energy distribution with the observational thresholds of telescopes determines the fraction of FRBs that can be detected by the telescopes. For a specific telescope survey, the observational number of FRBs in the redshift range ( $z_1, z_2$ ) or in the energy range ( $E_1, E_2$ ) can be calculated by

$$N = \mathcal{T} \frac{\mathcal{A}}{4\pi} f_b \int_{z_1}^{z_2} \dot{R}_m(z) \frac{dV(z)}{1+z} \left[ \int_{\max[E_{\text{th}}(z), E_{\min}] }^{E_{\max}} \Phi(E) dE \right], \quad (7)$$

or

$$N = \mathcal{T} \frac{\mathcal{A}}{4\pi} f_b \int_{E_1}^{E_2} \Phi(E) \left[ \int_0^{\min[z_h(E), z_{\max}]} \dot{R}_m(z) \frac{dV(z)}{1+z} \right] dE, \quad (8)$$

where  $\mathcal{T}$  is the duration of each pointing observation,  $\mathcal{A}$  is the sky area of the survey,  $f_b$  is the beaming factor of the FRB radiation,  $dV(z) = 4\pi d_c(z)^2 c H(z)^{-1} dz$  is the comoving volume element,  $d_c(z) = c \int_0^z H(z')^{-1} dz'$  is the comoving distance, and the factor  $(1+z)$  represents the cosmological time dilation for the observed rates. The energy threshold of a telescope involved in Equations (7) and (8) can be determined by

$$E_{\text{th}}(z) = 4\pi d_c(z)^2 (1+z) \Delta\nu \mathcal{F}_{\nu, \text{th}} k(z), \quad (9)$$

where  $\Delta\nu$  and  $\mathcal{F}_{\nu, \text{th}}$  are the frequency bandwidth and the fluence sensitivity of the telescope, respectively. The correction factor  $k(z)$  converts the FRB energy from the observational band ( $\nu_1, \nu_2$ ) into a common emitting frequency range ( $\nu_a, \nu_b$ ) for all FRBs. By assuming a power-law spectrum,  $\mathcal{F}_\nu \propto \nu^{-\beta}$ , the  $k$ -correction can be calculated to

$$k(z) = \frac{\nu_b^{(1-\beta)} - \nu_a^{(1-\beta)}}{[(1+z)\nu_2]^{(1-\beta)} - [(1+z)\nu_1]^{(1-\beta)}}. \quad (10)$$

Finally, the horizon redshift  $z_h(E)$  appearing in integral (8) can be solved from the equation  $E = E_{\text{th}}(z_h)$ , which means that, for

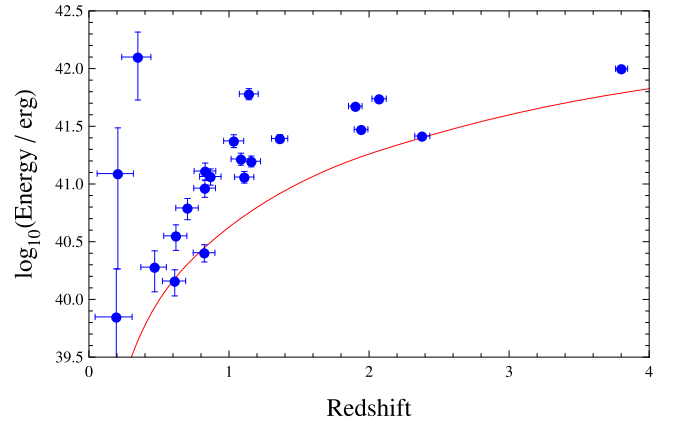


**Figure 2.** The 22 Parkes FRBs in the  $z$ - $E$  plane. The errors of the data correspond to the uncertain range of  $\text{DM}_{\text{host}}$  from zero to  $200 \text{ pc cm}^{-3}$  and the central values are given for  $\text{DM}_{\text{host}} = 100 \text{ pc cm}^{-3}$ . The FRB energies are corrected for a tentative spectral index  $\beta = 0.8$ . The solid line represents the observational energy threshold of the Parkes telescope below which the identification opportunity of an FRB decreases drastically.

an isotropic energy of FRBs, the observational horizon of the telescope is at  $z_h$ . The maximum redshift  $z_{\max}$  corresponds to the maximum DM below which the FRB searches were conducted. One must keep in mind that a remarkable number of FRBs of relatively high redshifts and of relatively low energies have been missed by the present telescope surveys due to the telescope thresholds, when the observational distributions of FRBs are discussed and used.

## 3. Fitting to Observational Distributions

Up to FRB 171209, a total of 30 FRBs have been detected by different telescopes including the Parkes, UTMOST, GBT, ASKAP, and Arecibo, which are cataloged on the website <http://frbcat.org/> (see Petroff et al. 2016 and references therein). In this paper, we only take into account the largest subsample provided by the Parkes containing 22 FRBs, so that the very different parameters of different telescopes will not be involved. The only repeated FRB 121102 discovered by Arecibo is just excluded. The redshifts of the FRBs can be inferred from their DMs, by subtracting the contributions from the Milky Way and the host galaxies, while the DM of the FRB sources are considered to be relatively much lower. Specifically, the following equation is used to calculate the redshifts of the FRBs (Inoue 2003; Ioka 2003; Deng & Zhang 2014):

$$\begin{aligned} \text{DM}_{\text{IGM}}(z) &= \text{DM} - \text{DM}_{\text{MW}} - \frac{\text{DM}_{\text{host}}}{1+z} \\ &= f_{\text{IGM}} f_e \frac{3cH_0\Omega_b}{8\pi Gm_p} \int_0^z \frac{H_0(1+z')}{H(z')} dz', \end{aligned} \quad (11)$$

where  $f_{\text{IGM}} \sim 0.83$  is the fraction of baryon mass in the intergalactic medium (IGM) and  $f_e \sim 7/8$  is the number ratio between free electrons and baryons (including proton and neutron) in IGM, which was first introduced by Deng & Zhang (2014),  $m_p$  is the proton mass, and  $\Omega_b = 0.04$ . While the values of  $\text{DM}_{\text{MW}}$  have been provided in the catalog, the  $\text{DM}_{\text{host}}$  are completely unknown. In any case, a rough estimation on the order of magnitude of  $\text{DM}_{\text{host}}$  could still be made by referring

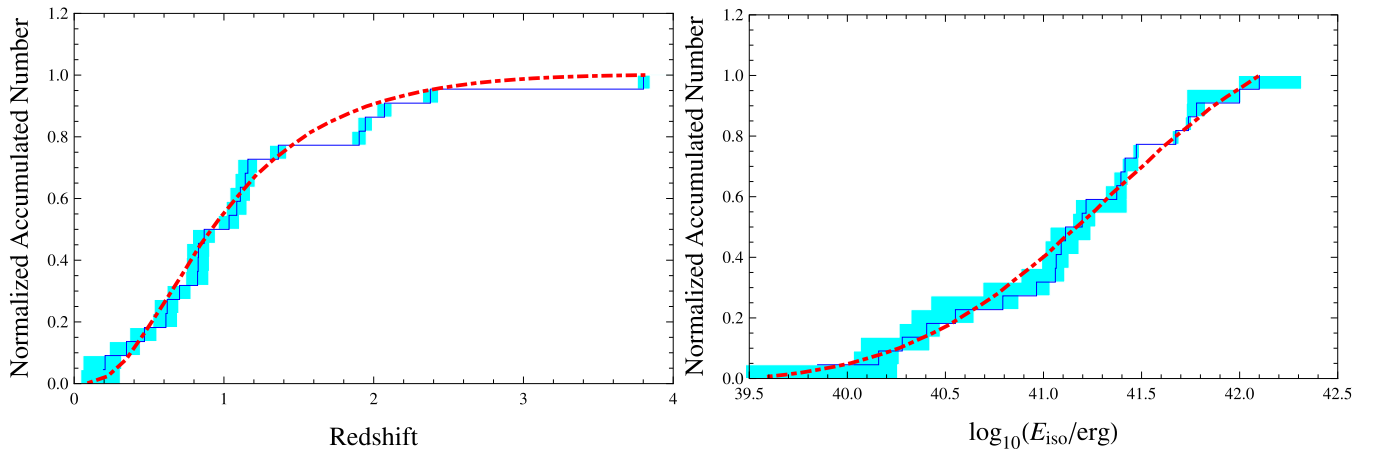


**Figure 3.** Normalized accumulated distributions in redshift (left) and isotropic energy (right) of the 22 Parkes FRBs. The solid line is obtained by fixing  $DM_{\text{host}}$  to  $100 \text{ pc cm}^{-3}$  for all FRBs, while the shadow represents the uncertainty of the FRB distribution arising from the variation of  $DM_{\text{host}}$  from 0 to  $200 \text{ pc cm}^{-3}$ . An example fitting by the CBM model to the FRB distribution for  $DM_{\text{host}} = 100 \text{ pc cm}^{-3}$  is presented by the dashed-dotted line, where the model parameters are taken as  $\beta = 0.8$ ,  $\gamma = 1.4$ , and  $\tau_c = 350 \text{ Myr}$ .

to the observation of the host galaxy of FRB 121102, which gives<sup>6</sup>  $DM_{\text{host}} \sim 100 \text{ pc cm}^{-3}$ , although it is not clear whether or not this repeated FRB has an origin identical to the nonrepeated ones. Therefore, in our calculations, we take the values of  $DM_{\text{host}}$  varying from zero to  $200 \text{ pc cm}^{-3}$ , where the upper bound is set according to the present minimum DM of the Parkes FRBs, i.e.,  $DM_{\text{FRB150807}} = 266.5 \text{ pc cm}^{-3}$ . This variation range of  $DM_{\text{host}}$  leads to the uncertainty of redshifts and energies of the FRBs, as shown in Figure 2.

With an inferred redshift, the isotropically equivalent energy of an FRB can be calculated by

$$E = 4\pi d_c(z)^2(1+z)\Delta\nu\mathcal{F}_\nu k(z), \quad (13)$$

where the Parkes parameters for  $k$ -correction are taken as follows:  $\nu_1 = 1182 \text{ MHz}$  and  $\nu_2 = 1522 \text{ MHz}$  (i.e.,  $\Delta\nu = 0.34 \text{ GHz}$  centering at  $1.35 \text{ GHz}$ ) and then  $\nu_a = 1182 \text{ MHz}$  and  $\nu_b = 7610 \text{ MHz}$ , which correspond to the redshift range of  $0 \lesssim z \lesssim 4$  of observed FRBs. For simplicity, a tentative spectral index  $\beta = 0.8$  is assumed in view of our very poor knowledge of the FRBs' spectra and the high degeneracy between  $\beta$  and  $\gamma$  due to the  $k$ -correction. Two Parkes FRBs have published spectral indices including FRB 131104 with  $\beta = 0.3 \pm 0.9$  (Ravi et al. 2015) and FRB 150418 with  $\beta = 1.3 \pm 0.5$  (Keane et al. 2016). However, it should be cautioned that these values are very sensitive to the true position of the FRBs within the telescope beam pattern. Finally, the energy threshold of the Parkes telescope, presented by the solid line in Figure 2, is calculated by Equation (9) with

a fluence sensitivity as (Bera et al. 2016; Caleb et al. 2016)

$$\mathcal{F}_{\nu,\text{th}} = 0.04S/N \left[ \frac{\Delta t_{\text{obs}}(z)}{1 \text{ ms}} \right]^{1/2} \text{ Jy ms}, \quad (14)$$

where the characteristic minimum signal-to-noise ratio is adopted to  $S/N = 10$  and the typical FRB duration  $\Delta t_{\text{obs}}(z)$  as a function of redshift is given by fitting the observational duration distribution as was done in Cao et al. (2017a).

In view of the limit number of observed FRBs, we only pay attention to the accumulated distributions of the 22 Parkes FRBs, as presented in Figure 3. These FRB distributions are somewhat uncertain due to the uncertainty of  $DM_{\text{host}}$ . For a fixed  $DM_{\text{host}}$ , we can fit the observational distributions by Equations (7) and (8) by varying the values of the most crucial model parameters, i.e.,  $\tau_c$  and  $\gamma$ . The goodness of the fits is assessed by the Kolmogorov–Smirnov test, where the observational uncertainties are not involved. Then, for a general consideration, we carry out such calculations for three different values of  $DM_{\text{host}}$ , i.e., 0, 100, and  $200 \text{ pc cm}^{-3}$ . As a result, the 95% confidence level regions of parameters  $\tau_c$  and  $\gamma$  are presented in Figure 4 by two contours deriving from the fittings of the redshift and energy distributions, respectively. The large overlap of the two contours demonstrates that sufficiently good fits of observations can easily be found in the CBM model. One example of the best fits to the distributions for  $DM_{\text{host}} = 100 \text{ pc cm}^{-3}$  is shown by the dashed-dotted line in Figure 3, which is given by  $\tau_c = 350 \text{ Myr}$ ,  $\gamma = 1.4$ , and  $E_{\text{min}} = 3 \times 10^{39} \text{ erg}$ . The results for different values of  $DM_{\text{host}}$  together indicate that, while  $1.2 \lesssim \gamma \lesssim 1.7$ , the characteristic delay time  $\tau_c$  can range from several tens to several hundreds of megayears,<sup>7</sup> which is broadly consistent with the theoretical expectations of the CBM model. This somewhat favors the CBM explanation of the FRB phenomena, although the range of  $\tau_c$  is still too large to fix the nature of the compact binaries.

Finally, by using the total FRB number of 22, we can determine the local rate of the FRB-related CBMs for different

<sup>6</sup> The DM of FRB 121102 contributed by its host galaxy was suggested by Tendulkar et al. (2017) to

$$DM_{\text{host,FRB121102}} \approx 324 \text{ pc cm}^{-3} \left[ \frac{4d_{\text{kpc}}f}{\zeta(1+\epsilon^2)} \right]^{1/2}, \quad (12)$$

where  $d_{\text{kpc}} = d/\text{kpc}$  is the total path length of the FRB emission through the galactic disk,  $f$  is the fraction of the path that is occupied by ionized clouds,  $\zeta \geq 1$  defines cloud-to-cloud density variations in the ionized regions,  $\epsilon \leq 1$  is the fractional variation inside discrete clouds due to turbulent-like density variations.

<sup>7</sup> If we release the fixing of the value of  $\beta$ , our constraints on the model parameters can be somewhat changed, in particular, for the parameter  $\gamma$  (Cao et al. 2017a) because of its tight connection with  $\beta$  through the  $k$ -correction of FRB energies. However, the value of  $\tau_c$  would not substantially deviate from the large range presented here.

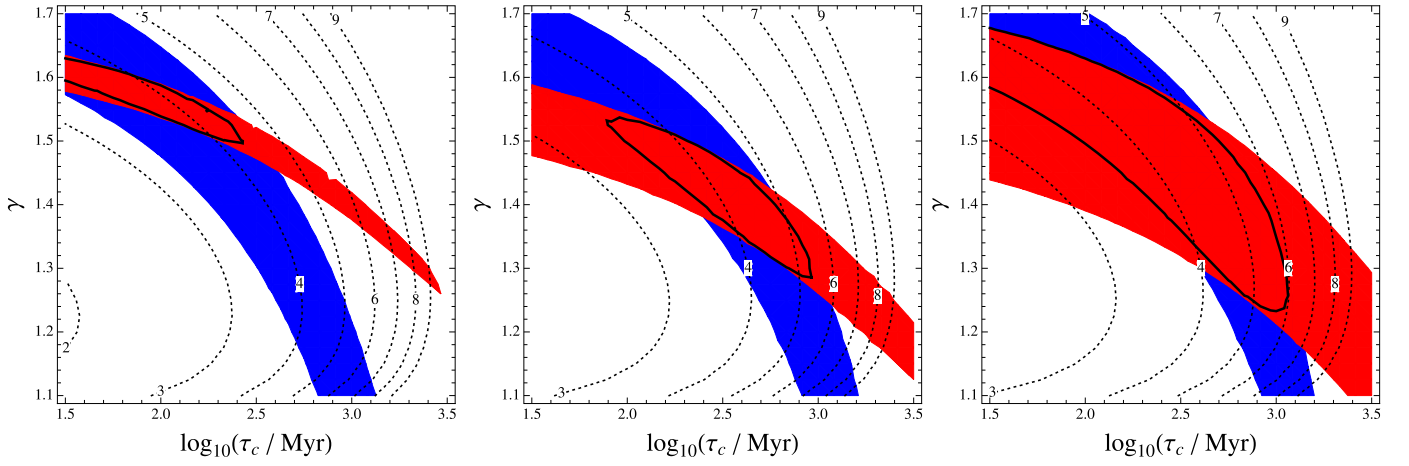


**Figure 4.** 95% confidence level contours of parameters  $\tau_c$  and  $\gamma$  given by the Kolmogorov–Smirnov test. The blue and red contours correspond to the fittings of redshift and energy distributions, respectively. The overlapped region of the contours is presented by the solid line. The dashed lines indicate the required local event rate of FRBs as labeled by  $\dot{R}_m(0)/10^4 \text{ Gpc}^{-3} \text{ yr}^{-1}$ . From left to right, the value of  $\text{DM}_{\text{host}}$  is fixed to 0  $\text{pc cm}^{-3}$ , 100  $\text{pc cm}^{-3}$ , and 200  $\text{pc cm}^{-3}$ , respectively.

values of  $\tau_c$  and  $\gamma$ , as labeled by the dashed lines in Figure 4. According to the overlapped regions of the contours for all different  $\text{DM}_{\text{host}}$  cases, we can have

$$\dot{R}_m(0) \approx (3\text{--}6) \times 10^4 \text{ Gpc}^{-3} \text{ yr}^{-1} f_b^{-1} \left( \frac{\mathcal{T}}{270 \text{ s}} \right)^{-1} \left( \frac{\mathcal{A}}{2\pi} \right)^{-1}, \quad (15)$$

where the reference values of  $\mathcal{T}$  and  $\mathcal{A}$  are taken by referring to Thornton et al. (2013). Substituting the above local event rate into Equation (1) and integrating  $\dot{R}_m(z)$  from  $z = 0$  to 4, we can obtain the full-sky event rates for different fluence sensitivities, as listed in Table 1, where  $\tau_c = 350 \text{ Myr}$ ,  $\gamma = 1.4$ , and  $\dot{R}_m(0) = 4.1 \times 10^4 \text{ Gpc}^{-3} \text{ yr}^{-1}$  are taken. For the sensitivity  $\mathcal{F}_{\nu, \text{th}} = 0.4 \text{ Jy ms}$  corresponding to the Parkes, the presented rate of 14,080  $\text{day}^{-1} \text{ sky}^{-1}$  can be easily understood by the following calculation:

$$\begin{aligned} \dot{R}_{\text{FRB, full-sky}} &= \frac{1}{f_b} \cdot \frac{N_{\text{FRB, Parkes}}}{\mathcal{T}} \cdot \frac{4\pi}{\mathcal{A}} \\ &= 14,080 \text{ day}^{-1} \text{ sky}^{-1} f_b^{-1} \left( \frac{\mathcal{T}}{270 \text{ s}} \right)^{-1} \left( \frac{\mathcal{A}}{2\pi} \right)^{-1}. \end{aligned} \quad (16)$$

#### 4. Conclusion and Discussions

The fitting results presented in this paper indicate that the CBM model with reasonable parameter values can account for the FRB phenomena accounting for the redshift dependence of the event rate; though, the uncertainty of model parameters is still large. It is at least indicated that the FRB rates could be connected with CSFRs by power-law distributed delay times and the FRB energy distribution could be effectively expressed by a single power law. Furthermore, the relatively certain value of the local event rate of FRBs enables us to discuss the nature of the compact binaries, specifically, two WDs, two NSs, or an NS and a BH.

Mergers of NS–NS and NS–BH binaries have long been considered to be progenitors of short GRBs; this was recently confirmed by the discovery of GRB 170817A and the

**Table 1**  
Full-sky FRB Event Rates for Different Sensitivities

$\mathcal{F}_{\nu, \text{th}}$ for $\Delta t_{\text{obs}} = 1 \text{ ms}$ (Jy ms)	Event Rate (Number/day/sky)
0.2	20,000
0.4	14,080
1.0	8100
3.0	3500

associated gravitational wave event GW 170817. On the one hand, according to GW 170817, the rate of NS–NS mergers has been directly inferred to  $\dot{R}_{\text{ns-ns}}(0) \sim 1540_{-1220}^{+3200} \text{ Gpc}^{-3} \text{ yr}^{-1}$  (Abbott et al. 2017). An absolute upper limit on this rate was previously imposed to 12,600  $\text{Gpc}^{-3} \text{ yr}^{-1}$  by the nondetection of this type of mergers during O1 of LIGO (Abbott et al. 2016). On the other hand, during the past decade, the local event rate of short GRBs has been widely investigated and found to be from a few to a few tens of  $\text{Gpc}^{-3} \text{ yr}^{-1}$  (Guetta & Piran 2006; Nakar et al. 2006; Guetta & Stella 2009; Dietz 2011; Coward et al. 2012; Wanderman & Piran 2015; Tan et al. 2018; Zhang & Wang 2018). According to the latest statistics, we can obtain  $\dot{R}_{\text{sGRB}}(0) \approx 4 \text{ Gpc}^{-3} \text{ yr}^{-1}$  for an assumed minimum luminosity of short GRBs of  $L_{\text{min}} \sim 5 \times 10^{49} \text{ erg s}^{-1}$ . The conversion of this short GRB event rate to merger rate is highly dependent on the measurements of opening angles of GRB jets. For a possible range of the angles of  $5^\circ\text{--}30^\circ$ , the local merger rate can be inferred to  $\dot{R}_{\text{ns-ns}}(0) \sim (30\text{--}1100) \text{ Gpc}^{-3} \text{ yr}^{-1}$ , which is broadly in agreement with the LIGO result. Meanwhile, the rate of NS–BH mergers is considered to be comparable to or more likely lower than the rate of NS–NS mergers (Abadie et al. 2010). Therefore, it seems difficult to explain all FRBs by only NS–NS and NS–BH mergers (see Callister et al. 2016).

Mergers of double WDs could lead to different outcomes, including SN Ia explosions, a stable WD, and a stable NS through accretion-induced collapse (AIC; Canal & Schatzman 1976; Nomoto & Kondo 1991). Simulations showed that the local rate of WD mergers can reach several times  $10^4 \text{ Gpc}^{-3} \text{ yr}^{-1}$  (Badenes & Maoz 2012), which was supported by the measurement of SN Ia rate as  $(3.01 \pm 0.062) \times 10^4 \text{ Gpc}^{-3} \text{ yr}^{-1}$  (Li et al. 2011); though, SNe Ia can also originate from a single WD accreting from its companion star. The general consistency between the WD

merger rate and the rate presented in Equation (15), if the beaming of the FRB radiation can be ignored, indicates that the WD mergers could be the most promising origin of FRBs in the CBM scenario. So far, there was no bright SN Ia reported to be associated with observed FRBs. Therefore, the plausible origin of FRBs is the formation of a massive WD as suggested by Kashiyama et al. (2013) or a stable AIC NS. Here, the fraction of AICs of WD–WD mergers is not clear (e.g., Yungelson & Livio 1998). If a remarkable amount of  $r$ -process elements can be synthesized during AICs (Wheeler et al. 1998), the AIC rate would be constrained to be at least an order of magnitude lower than  $\sim 10^4 \text{ Gpc}^{-3} \text{ yr}^{-1}$  to be consistent with the observed abundances of neutron-rich elements in the universe (Fryer et al. 1999).

In any case, by considering the possible high beaming of FRB radiation (i.e.,  $f_b \ll 1$ ), the inferred extremely high rate of FRBs could be a serious problem for any kind of CBMs. A possible solution of this problem is that FRBs could actually be produced by the merger products but not by the mergers themselves and, furthermore, the FRBs are all repeated just on a timescale longer than the period (i.e., several years) of current observations. If the merger products can produce an FRB on an average timescale of  $t_v$  during an activity period of  $nt_v$ , then the rate presented in Equation (15) can be reduced by a factor of  $n$ . In this case, a rapidly rotating and highly magnetized NS as a merger product could be most favorable for causing repeatable FRB radiation. This discussion is applicable for the WD AICs and also for NS–NS mergers. In the latter case, the formation of a massive NS is usually suggested by the afterglow emission of short GRBs (Dai et al. 2006; Fan & Xu 2006; Rowlinson et al. 2013) and even by the kilonova emission (e.g., Yu & Dai 2017). In the framework of the merger-produced NS model, the young NS could power FRBs by its rotational energy as super-giant radio pulses of pulsars (e.g., Connor et al. 2016; Cordes & Wasserman 2016; Lyutikov 2017) or by its magnetic energy as the giant flares of Galactic magnetars (e.g., Popov & Postnov 2010; Kulkarni et al. 2014; Katz 2016b). Additionally, a persistent counterpart associated with the FRBs can be expected to arise from the interaction of the merger/AIC ejecta with the environmental materials (e.g., Murase et al. 2016; Piran et al. 2013; Piro & Kulkarni 2013). These characteristics could make regular FRBs similar to the repeated FRB 121102 (Cao et al. 2017b; Dai et al. 2017; Kashiyama & Murase 2017; Metzger et al. 2017; Michilli et al. 2018), which needs to be investigated in the future.

The authors thank Bo Wang and Fa-Yin Wang for valuable discussions. This work is supported by the National Natural Science Foundation of China (grant Nos. 11473008 and 11373006).

### ORCID iDs

Yun-Wei Yu  <https://orcid.org/0000-0002-1067-1911>

### References

- Abadie, J., Abbott, B. P., Abbott, R., et al. 2010, *CQGra*, 27, 173001
- Abbott, B. P., Abbott, R., Abbott, T. D., et al. 2016, *PhRvL*, 116, 061102
- Abbott, B. P., Abbott, R., Abbott, T. D., et al. 2017, *PhRvL*, 119, 161101
- Badenes, C., & Maoz, D. 2012, *ApJL*, 749, L11
- Bannister, K. W., Shannon, R. M., Macquart, J.-P., et al. 2017, *ApJL*, 841, L12
- Bauswein, A., Goriely, S., & Janka, H.-T. 2013, *ApJ*, 773, 78
- Belczynski, K., Kalogera, V., & Bulik, T. 2002, *ApJ*, 572, 407
- Belczynski, K., Perna, R., Bulik, T., et al. 2006, *ApJ*, 648, 1110
- Bera, A., Bhattacharyya, S., Bharadwaj, S., Bhat, N. D. R., & Chengalur, J. N. 2016, *MNRAS*, 457, 2530
- Bouwens, R. J., Illingworth, G. D., Oesch, P. A., et al. 2012, *ApJ*, 754, 83
- Bouwens, R. J., Illingworth, G. D., Oesch, P. A., et al. 2015, *ApJ*, 803, 34
- Burke-Spolaor, S., & Bannister, K. W. 2014, *ApJ*, 792, 19
- Caleb, M., Flynn, C., Bailes, M., et al. 2016, *MNRAS*, 458, 708
- Caleb, M., Flynn, C., Bailes, M., et al. 2017, *MNRAS*, 468, 3746
- Callister, T., Kanner, J., & Weinstein, A. 2016, *ApJL*, 825, L12
- Canal, R., & Schatzman, E. 1976, *A&A*, 46, 229
- Cao, X.-F., Xiao, M., & Xiao, F. 2017a, *RAA*, 17, 14
- Cao, X.-F., & Yu, Y.-W. 2018, *PhRvD*, 97, 023022
- Cao, X.-F., Yu, Y.-W., & Dai, Z.-G. 2017b, *ApJL*, 839, L20
- Champion, D. J., Lorimer, D. R., McLaughlin, M. A., et al. 2004, *MNRAS*, 350, L61
- Champion, D. J., Petroff, E., Kramer, M., et al. 2016, *MNRAS*, 460, L30
- Chary, R., Berger, E., & Cowie, L. 2007, *ApJ*, 671, 272
- Chatterjee, S., Law, C. J., Wharton, R. S., et al. 2017, *Natur*, 541, 58
- Chruslinska, M., Belczynski, K., Klencki, J., & Benacquista, M. 2018, *MNRAS*, 474, 2937
- Coe, D., Umetsu, K., Zitrin, A., et al. 2012, *ApJ*, 757, 22
- Connor, L., Sievers, J., & Pen, U.-L. 2016, *MNRAS*, 458, L19
- Cordes, J. M., & Wasserman, I. 2016, *MNRAS*, 457, 232
- Coulter, D. A., Foley, R. J., Kilpatrick, C. D., et al. 2017, *Sci*, 358, 1556
- Coward, D. M., Howell, E. J., Piran, T., et al. 2012, *MNRAS*, 425, 2668
- Dai, Z. G., Wang, J. S., & Yu, Y. W. 2017, *ApJL*, 838, L7
- Dai, Z. G., Wang, X. Y., Wu, X. F., & Zhang, B. 2006, *Sci*, 311, 1127
- Deng, W., & Zhang, B. 2014, *ApJL*, 783, L35
- Dietz, A. 2011, *A&A*, 529, A97
- Eichler, D., Livio, M., Piran, T., & Schramm, D. N. 1989, *Natur*, 340, 126
- Evans, P. A., Cenko, S. B., Kennea, J. A., et al. 2017, *Sci*, 358, 1565
- Fan, Y.-Z., & Xu, D. 2006, *MNRAS*, 372, L19
- Fialkov, A., & Loeb, A. 2017, *ApJL*, 846, L27
- Fryer, R. J., Benz, W., Herant, M., & Colgate, S. A. 1999, *ApJ*, 516, 892
- Graur, O., & Maoz, D. 2013, *MNRAS*, 430, 1746
- Greggio, L. 2005, *A&A*, 441, 1055
- Guetta, D., & Piran, T. 2006, *A&A*, 453, 823
- Guetta, D., & Stella, L. 2009, *A&A*, 498, 329
- Hao, J.-M., & Yuan, Y.-F. 2013, *A&A*, 558, A22
- Hopkins, A. M., & Beacom, J. F. 2006, *ApJ*, 651, 142
- Hotkezaka, K., Kiuchi, K., Kyutoku, K., et al. 2013, *PhRvD*, 87, 024001
- Inoue, A. K. 2003, *PASJ*, 55, 901
- Ioka, K. 2003, *ApJL*, 598, L79
- Ishida, E. E. O., de Souza, R. S., & Ferrara, A. 2011, *MNRAS*, 418, 500
- Just, O., Bauswein, A., Pulpillo, R. A., Goriely, S., & Janka, H.-T. 2015, *MNRAS*, 448, 541
- Kashiyama, K., Ioka, K., & Mészáros, P. 2013, *ApJL*, 776, L39
- Kashiyama, K., & Murase, K. 2017, *ApJL*, 839, L3
- Katz, J. I. 2016a, *ApJ*, 818, 19
- Katz, J. I. 2016b, *ApJ*, 826, 226
- Keane, E. F., Johnston, S., Bhandari, S., et al. 2016, *Natur*, 530, 453
- Keane, E. F., Stappers, B. W., Kramer, M., & Lyne, A. G. 2012, *MNRAS*, 425, L71
- Kistler, M. D., Yüksel, H., Beacom, J. F., Hopkins, A. M., & Wytke, J. S. B. 2009, *ApJL*, 705, L104
- Kulkarni, S. R., Ofek, E. O., Neill, J. D., Zheng, Z., & Juric, M. 2014, *ApJ*, 797, 70
- Lattimer, J. M., & Schramm, D. N. 1974, *ApJL*, 192, L145
- Lawrence, E., Vander Wiel, S., Law, C., et al. 2017, *AJ*, 154, 117
- Li, L.-B., Huang, Y.-F., Zhang, Z.-B., Li, D., & Li, B. 2017, *RAA*, 17, 6
- Li, L.-X., & Paczyński, B. 1998, *ApJL*, 507, L59
- Li, W., Chornock, R., Leaman, J., et al. 2011, *MNRAS*, 412, 1473
- Liu, T., Romero, G. E., Liu, M.-L., & Li, A. 2016, *ApJ*, 826, 82
- Lorimer, D. R., Bailes, M., McLaughlin, M. A., Narkevic, D. J., & Crawford, F. 2007, *Sci*, 318, 777
- Lu, W. B., & Kumar, P. 2016, *MNRAS*, 461, L122
- Lyutikov, M. 2017, *ApJL*, 838, L13
- Macquart, J.-P., & Ekers, R. D. 2018, *MNRAS*, 474, 1900
- Maoz, D., & Mannucci, F. 2012, *PASA*, 29, 447
- Marcote, B., Paragi, Z., Hessels, J. W. T., et al. 2017, *ApJL*, 834, L8
- Masui, K., Lin, H.-H., Sievers, J., et al. 2015, *Natur*, 528, 523
- McLeod, D. J., McLure, R. J., & Dunlop, J. S. 2016, *MNRAS*, 459, 3812
- Mennekens, N., & Vanbeveren, D. 2016, *A&A*, 589, A64
- Mennekens, N., Vanbeveren, D., De Greve, J. P., & De Donder, E. 2010, *A&A*, 515, A89

- Metzger, B. D., Berger, E., & Margalit, B. 2017, *ApJ*, **841**, 14
- Metzger, B. D., Martínez-Pinedo, G., Darbha, S., et al. 2010, *MNRAS*, **406**, 2650
- Michilli, D., Seymour, A., Hessels, J. W. T., et al. 2018, *Natur*, **553**, 182
- Mingarelli, C. M. F., Levin, J., & Lazio, T. J. W. 2015, *ApJL*, **814**, L20
- Murase, K., Kashiyama, K., & Mészáros, P. 2016, *MNRAS*, **461**, 1498
- Nakar, E., Gal-Yam, A., & Fox, D. B. 2006, *ApJ*, **650**, 281
- Nomoto, K., & Kondo, Y. 1991, *ApJL*, **367**, L19
- Oesch, P. A., Bouwens, R. J., Illingworth, G. D., et al. 2013, *ApJ*, **773**, 75
- Oesch, P. A., Bouwens, R. J., Illingworth, G. D., et al. 2014, *ApJ*, **786**, 108
- Oppermann, N., Connor, L. D., & Pen, U.-L. 2016, *MNRAS*, **461**, 984
- Paczynski, B. 1986, *ApJL*, **308**, L43
- Petroff, E., Barr, E. D., Jameson, A., et al. 2016, *PASA*, **33**, e045
- Petroff, E., Burke-Spolaor, S., Keane, E. F., et al. 2017, *MNRAS*, **469**, 4465
- Piran, T. 1992, in AIP Conf. Ser. 272, Proceedings of the XXVI International Conference on High Energy Physics, ed. J. R. Sanford (Melville, NY: AIP), 1626
- Piran, T., Nakar, E., & Rosswog, S. 2013, *MNRAS*, **430**, 2121
- Piro, A. L., & Kulkarni, S. R. 2013, *ApJL*, **762**, L17
- Popov, S. B., & Postnov, K. A. 2010, in Evolution of Cosmic Objects through their Physical Activity, Proceedings of the Conference dedicated to Viktor Ambartsumian's 100th Anniversary, ed. H. A. Harutyunian, A. M. Mickaelian, & Y. Terzian (Yerevan: NAS RA), 129
- Portegies Zwart, S. F., & Yungelson, L. R. 1998, *A&A*, **332**, 173
- Ravi, V., Shannon, R. M., & Jameson, A. 2015, *ApJL*, **799**, L5
- Rowlinson, A., O'Brien, P. T., Metzger, B. D., Tanvir, N. R., & Levan, A. J. 2013, *MNRAS*, **430**, 1061
- Ruiter, A. J., Belczynski, K., Sim, S. A., et al. 2011, *MNRAS*, **417**, 408
- Spitler, L. G., Cordes, J. M., Hessels, J. W. T., et al. 2014, *ApJ*, **790**, 101
- Tan, W.-W., Cao, X.-F., & Yu, Y.-W. 2015, *NewA*, **38**, 11
- Tan, W.-W., Fan, X.-L., & Wang, F. Y. 2018, *MNRAS*, **475**, 1331
- Tendulkar, S. P., Bassa, C. G., Cordes, J. M., et al. 2017, *ApJL*, **834**, L7
- Thornton, D., Stappers, B., Bailes, M., et al. 2013, *Sci*, **341**, 53
- Totani, T. 2013, *PASJ*, **65**, L12
- Totani, T., Morokuma, T., Oda, T., Doi, M., & Yasuda, N. 2008, *PASJ*, **60**, 1327
- Tutukov, A. V., & Yungelson, L. R. 1981, *NInfo*, **49**, 3
- Vedantham, H. K., Ravi, V., Hallinan, G., et al. 2016, *ApJ*, **830**, 75
- Virgili, F. J., Zhang, B., Nagamine, K., & Choi, J.-H. 2011, *MNRAS*, **417**, 3025
- Wanderman, D., & Piran, T. 2015, *MNRAS*, **448**, 3026
- Wang, B., & Han, Z. 2012, *NewAR*, **56**, 122
- Wang, F. Y. 2013, *A&A*, **556**, A90
- Wang, F. Y., & Dai, Z. G. 2009, *MNRAS*, **400**, L10
- Wang, J.-S., Yang, Y.-P., Wu, X.-F., Dai, Z.-G., & Wang, F.-Y. 2016, *ApJL*, **822**, L7
- Webbink, R. F. 1984, *ApJ*, **277**, 355
- Wheeler, J. C., Cowan, J. J., & Hillebrandt, W. 1998, *ApJ*, **493**, L101
- Yamasaki, S., Totani, T., & Kiuchi, K. 2017, arXiv:1710.02302
- Yang, Y. P., & Zhang, B. 2017a, arXiv:1712.02702
- Yang, Y. P., & Zhang, B. 2017b, *ApJ*, **847**, 22
- Yu, Y.-W., Cheng, K. S., Chu, M. C., & Yeung, S. 2012, *JCAP*, **7**, 023
- Yu, Y.-W., Cheng, K.-S., Shiu, G., & Tye, H. 2014, *JCAP*, **11**, 040
- Yu, Y.-W., & Dai, Z.-G. 2017, arXiv:1710.01898
- Yu, Y.-W., Zhang, B., & Gao, H. 2013, *ApJL*, **776**, L40
- Yüksel, H., Kistler, M. D., Beacom, J. F., & Hopkins, A. M. 2008, *ApJL*, **683**, L5
- Yungelson, L., & Livio, M. 1998, *ApJ*, **497**, 168
- Zhang, B. 2016, *ApJL*, **827**, L31
- Zhang, G. Q., & Wang, F. Y. 2018, *ApJ*, **852**, 1